Journal of Alloys and Compounds, 211/212 (1994) 147–151
JALCOM 129

Internal friction and modulus defect in α-Fe-based, high-alloyed (Cr, Mo) hidamets

Igor S. Golovin
Moscow State Aircraft Technology University, Petrovka 27, Moscow 103767 (Russian Federation)

Abstract

The influence of heat treatment on the internal friction (IF) and modulus defect (DM) of high chromium ferritic alloys and α-Fe has been examined. The mechanisms of formation of magnetoelastic and dislocation hysteresis have been investigated. Temperature ranges and critical points associated with different damping mechanisms have been established.

1. Introduction

High chromium steels are of great interest due to their favourable combination of mechanical, corrosion and damping properties. Their position among other metallic materials is shown in Table 1, which combines information on the intrinsic damping capacity and the main mechanism of damping ($\Psi = \Delta W(A)/W(A) \approx 2\pi Q^{-1}$, where $\Delta W(A)$ is the dissipated and $W(A)$ the stored energy, A is the amplitude of deformation and Q^{-1} is the internal friction (IF); the damping index $\Psi_{0.1}$ is Ψ at $\sigma = 0.1\sigma_{0.2}$, where $\sigma_{0.2}$ is the yield stress. Good, stable mechanical properties and damping capacity are necessary for use over a wide temperature range.

TABLE 1. Intrinsic damping capacity of some metals and alloys

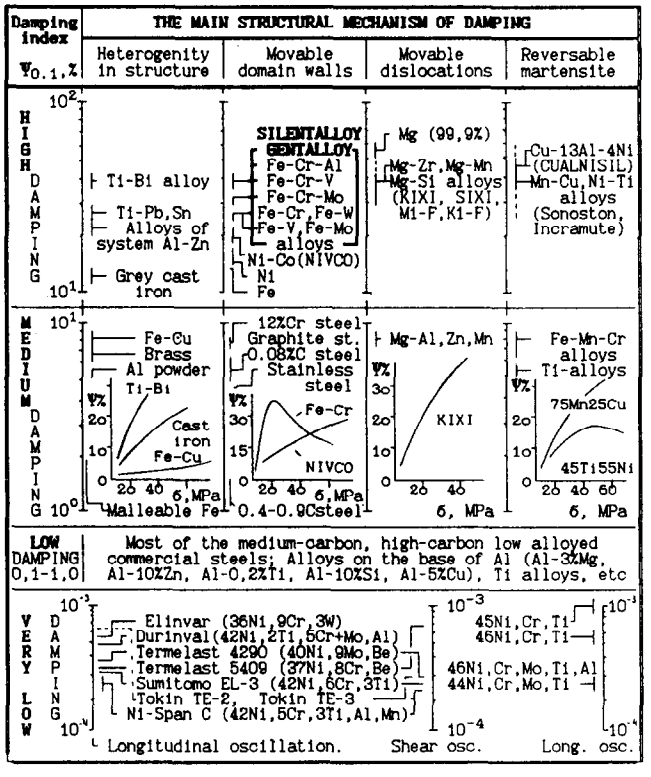

2. Experimental procedure

Armco Fe and several b.c.c. alloys with a Cr content in the range 11–25 wt.% and Mo content in the range 0–6 wt.% were used. Measurements of the amplitude and temperature dependence of IF (ADIF and TDIF) and the modulus defect (DM) were made on wire specimens in the amplitude range 1×10^{-5} to 140×10^{-5}, with a frequency of approximately 1 Hz and a magnetic field from zero to $H_S = 24\times10^3$ A m^{-1}, using an inverted torsion pendulum. An X-ray study was carried out using a DRON 2.0 apparatus. Small-angle scattering (SAS) of monochromatic neutrons (wavelength, 0.186 nm) was investigated using a neutron diffractometer "RAWAR"; tensile tests were performed using an "Instron" machine. Structural investigations were carried out using transmission electron microscopy: 3MB-100 with carbon replicas and JSM-7A with disc foils.

3. Experimental results

Increasing the annealing temperature (T_a) of cold-worked wire specimens of α-Fe and Cr16 and Cr16Mo4 steels leads to a non-monotonic change in IF, shear modulus defect ($\Delta f^2/f^2$), magnetic susceptibility ($\chi = B/I$) and coercive force H_C (Fig. 1). The dislocation (Q_d^{-1} at H_S) and magnetomechanical ($Q_h^{-1} = Q^{-1} - Q_d^{-1}$)

Elsevier Science S.A.
SSDI 0925-8388(94)00129-Z

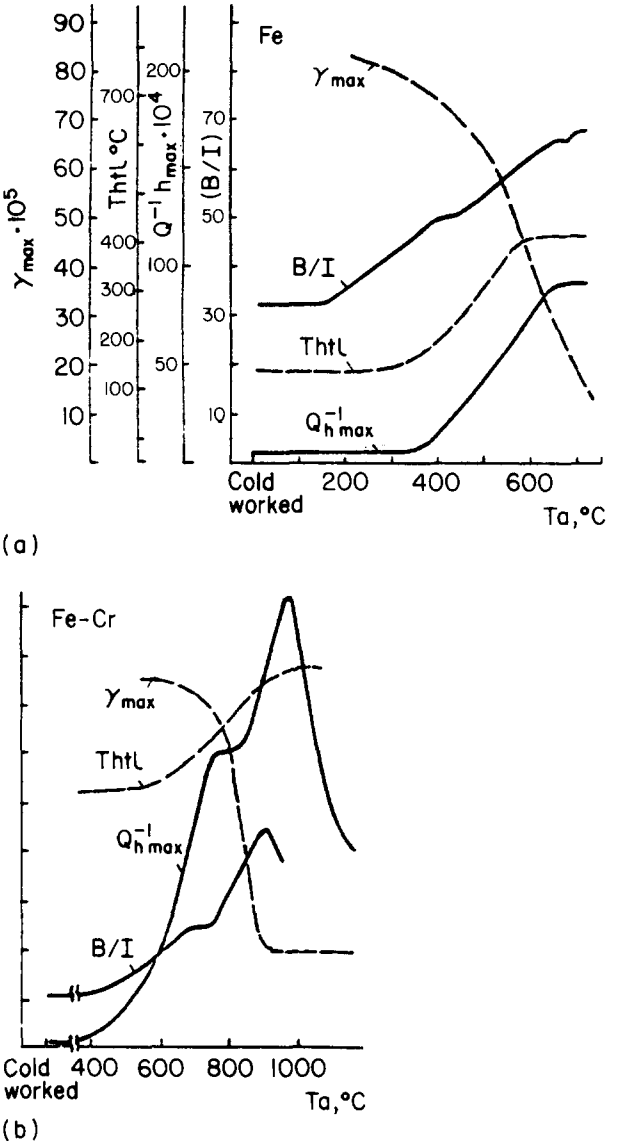

Fig. 1. The influence of the annealing temperature (T_a) of cold-worked samples of α-Fe (a) and Cr16 (b) steel on the IF level $Q_h^{-1}/(H=0)$, the location of maximum IF ($\gamma_{Q,max}$), the temperature of increase of the high-temperature background (T_{htb}) and the magnetic susceptibility (B/I).

parts of ADIF depend differently on T_a. A T_a value of about 950 °C for Cr16-type steels leads to a maximum of $Q_h^{-1}(T_a)$, $\Delta f^2/f^2(T_a)$ and $B/I(T_a)$ and a minimum of $H_C(T_a)$, independent of the cooling rate, and to a decrease in the amplitude location of the maximum γ_Q (for $Q_{h,max}^{-1}$) and γ_f (for f_{min}^2) and an increase in the temperature of the beginning of the high-temperature background (T_{htb}) at TDIF. The same character of Q_h^{-1} *vs.* γ was obtained for α-Fe in the ferrite range. The value of Q_h^{-1} changes correspondingly to χ. In the same temperature range, low values of H_C and dislocation density ρ_d are observed. The increase in T_a and τ_a leads to a monotonic increase in the grain size (GS) (see Table 2).

The values of Q_{max}^{-1} and $\Delta f_{max}^2/f^2$ decrease monotonically with an increase in the temperature of measurement (T_m) from −196 to 500 °C (Fig. 2). Dislocation IF (Q_d^{-1}) and subsequent dislocation DM ($\Delta f_d^2/f^2$) are negligibly small and practically constant in the temperature range −196–400 °C. The maxima on the curves $Q^{-1}(T_m)$ and $\Delta f^2/f^2(T_m)$ are observed in the range 500–650 °C. These maxima are associated with the dislocation part of the dissipated energy only. The amplitude location of the magnetomechanical IF(γ_Q) and DM(γ_f) maxima decreases with increasing T_m. The ratio $\gamma_Q/\gamma_f \approx 0.7$ is practically constant at the investigated temperatures below the Curie point (T_C). The increase in T_m above T_C leads to a subsequent increase in the Q^{-1} and f^2 values due to the dislocation microplasticity only. The IF level at ambient temperatures was found to be larger after preliminary measurements at 400 °C and above than after initial heat treatment only (Fig. 2(a)), *i.e.* additional annealing may be used to increase the damping capacity. The influence of the chemical composition on the damping capacity and mechanical properties of investigated steels has been described in ref. 1.

From the initial stages of ADIF(H_S), the temperature dependence of a microyield stress (corresponding to the level of dislocation strain $\gamma Q_d^{-1} = 10^{-7}$) was evaluated according to ref. 2. This temperature dependence was compared with $\frac{1}{2}\sigma_{0.2}$ *vs.* T_m and a satisfactory agreement in relative units was observed. Thus a similarity between the temperature dependences of the microyield and macroyield stresses is observed at elevated T_m and H_S field.

The amplitude hysteresis was investigated by comparison of the value of Q_0^{-1} at the deformation minimum (γ_0) after preliminary torsion deformation (γ_{pr}) (Fig. 3). The measurement of the Q_0^{-1} values was carried out after different γ_{pr} values ($\gamma_{pr} > \gamma_0$) after the decay of mechanical oscillations from γ_{pr} to γ_0 and during the next 10 min according to ref. 3. Three characteristic ranges on $Q_0^{-1}(\gamma_{pr})$ curves were established: the first is amplitude independent ($\gamma = 10^{-7}$–10^{-4}); the second is a range of increasing Q_0^{-1} *vs.* γ_{pr}; in the third, the values of Q_0^{-1} decrease *vs.* γ_{pr} (Fig. 4(a)); γ_{cr2} was measured under H_S and was found to be about 6×10^{-4}. The increase in the preliminary deformation into the range of microdeformation and plastic deformation (compared with the yield point) leads to suppression of the damping capacity of ferritic alloys (upper right in Fig. 4(a)). The same qualitative character has the influence of a static tensile stress (σ_{st}) on the IF level (Fig. 4(b)): the value of IF increases under the applied σ_{st} and after $\sigma_{st} \approx 2.5$ MPa it decreases. Using Meson's-type ultrasonic resonance equipment ($f_r \approx 21$ kHz), the influence of preliminary oscillations before measurements "N" (from 1×10^7 to 2×10^7) on the IF and DM

TABLE 2. Influence of T_a on various parameters

T_a (°C)	<800	900	1000	1100
D (μm)	Cold worked	15 (0.5 h); 22 (2 h)	25 (0.5 h); 30 (2 h)	45 (0.5 h)
	ρ_d=24 (c/w)	Annealing: 0.2 (0.5 h)		
$\rho_d \times 10^9$ (cm^{-2})	7.3	Quenching: 8 (0.5)	8.8 (0.5); 5.3 (2)	3.5 (0.5)
$H_C \times 100$ (A m^{-1})	>20	9 (q); 7 (a)	7 (q); 3 (a)	7 (q); 3.5 (a)

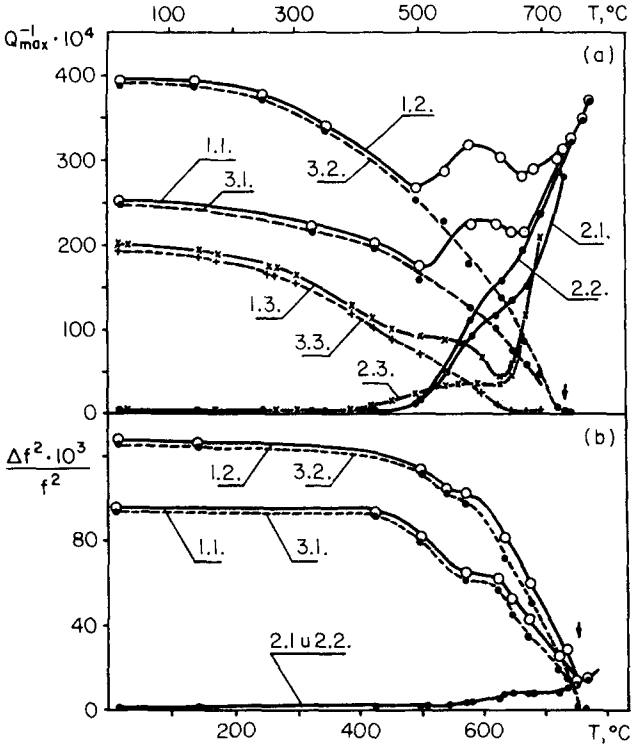

Fig. 2. The influence of the temperature of measurement (T_m) of the annealed samples on Q^{-1} (1.n), Q_h^{-1} (3.n) and Q_d^{-1} (2.n) (a) and $\Delta f^2/f^2$ (1.n), $\Delta f_h^2/f_h^2$ (3.n) and $\Delta f_d^2/f_d^2$ (2.n) (b) for Cr16 after T_a=1000 °C (n=1) and T_a=1000+680 °C (n=2) and for Cr16Mo4 (n=3).

values was obtained (Fig. 4(c)); this confirms the same non-monotonic influence of "N" at the $Q_h^{-1}(\gamma \leqslant \gamma_{pr})$ and $Q_d^{-1}(\gamma \geqslant \gamma_{pr})$ levels.

The value ΔQ_0^{-1} depends strongly on T_m and τ_m (Fig. 5): the initial values of Q_0^{-1} may be restored by annealing, and the degree and speed of restoration increase with T_m and τ_m. $\Delta Q_0^{-1}(\tau_m \to 0)$ increases with decreasing T_m at γ=constant (Fig. 5(a)). This regularity is associated with the decrease in the yield stress $\sigma_{0.2}$ and τ_{cr2} with increasing T_m (Fig. 5(b)). All regularities shown in Fig. 5 for ΔQ_0^{-1} were established for a modulus defect ($\Delta f^2/f_o^2$) and residual deformation γ_r after unloading.

4. Discussion

Damping in iron-based ferritic alloys occurs due to the additional magnetostriction deformation (ϵ_h):

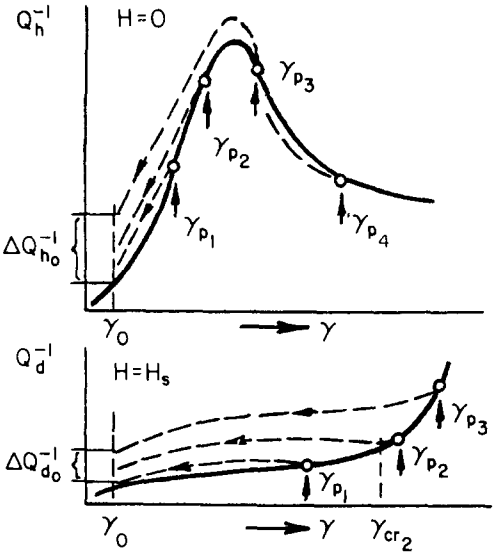

Fig. 3. (a) The scheme of measurement of ΔQ_0^{-1} and $\tau_{cr2}=G\gamma_{pr2}$. (b) The influence on ΔQ_0^{-1} (Cr16Mo4) of γ_{pr}.

$\epsilon = \epsilon_{el} + \epsilon_h$, where the ϵ_h value is proportional to the saturation magnetostriction constant (λ_S) and depends on the magnetic susceptibility (χ). These effects are mainly the result of the irreversible motion of the non-180° domain walls (DWs). The value of ϵ_h greatly depends on the chemical composition and heat treatment of the alloys. In binary annealed Fe–Cr alloys, the maximum values of $\delta = 2Q_h^{-1}$ and λ_S were observed at 15–16 wt.% Cr (see Table 3).

The internal stress level σ_i can be calculated from the $Q_{max}^{-1}(\gamma)$ position. As a first approximation, it is possible to use the relation $\sigma_{max}=0.7256\times\sigma_i$ [4], where σ_{max} may be taken from the strain position of the $Q_{max}^{-1}(\gamma)$ maximum; σ_i was found to be 15–20 MPa after furnace cooling. This is in good agreement with σ_i from X-ray experiments and residual stress relaxation tests ($\sigma_i \approx 18$ MPa). For a Maxwell distribution of internal stresses, the value of $\delta_{h,max}$ may be described by the equations

$$\begin{aligned} \delta_{h,max} &= 0.34k\lambda_S E/\sigma_i \quad (\text{at } \sigma \approx \sigma_{max}) \\ \delta_{h,max} &= 4k\lambda_S E/3\sigma \quad (\text{at } \sigma \ll \sigma_{max}) \end{aligned} \tag{1}$$

where $k \approx 1$ is a constant characteristic of the shape of the hysteresis loop, λ_S is the linear magnetostriction constant and E is the normal modulus of elasticity. Therefore it is possible to use the subsequent per-

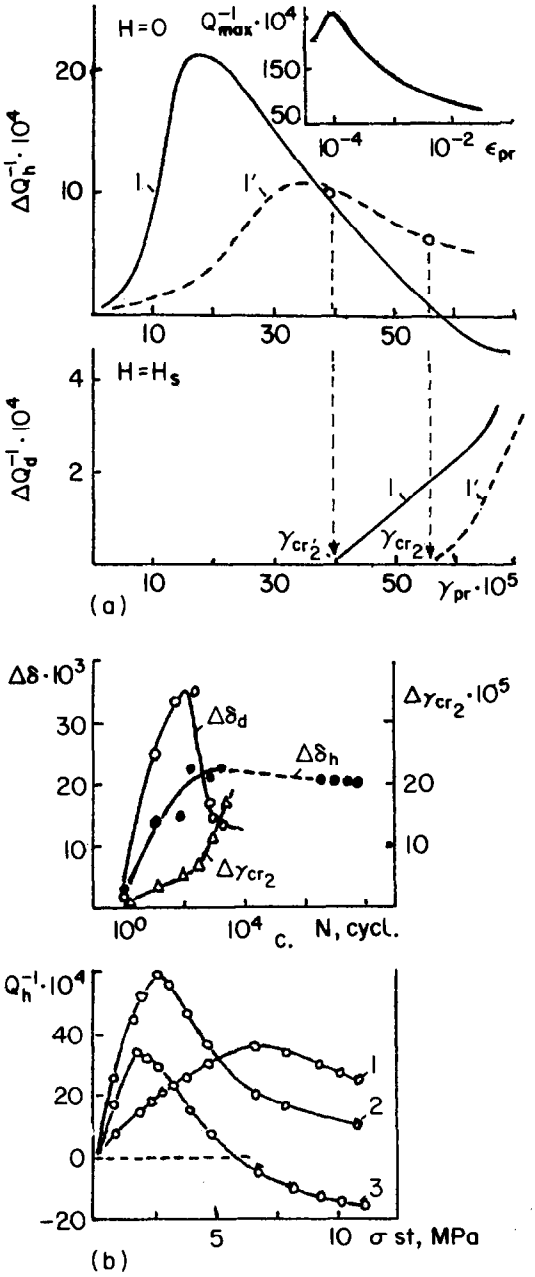

Fig. 4. The influence of γ_{pr} (a), σ_{st} (1–10, 2–20 and 2–30 MPa) (b) and N (c) (Cr16Mo4) on IF parameters.

formances of a substitutional solution ($\Delta\sigma_s$), dislocation ($\Delta\sigma_d$), dispersive hardening by coherent ($\Delta\sigma_c$) and non-coherent ($\Delta\sigma_{nc}$) precipitates and grain boundary ($\Delta\sigma_{gb}$) hardening for a determination of the logarithmic decrement in the same conditions. Finally, for IF [5, 6]

$$\delta_{h(s)} \approx 1/\left(\sum_{i=1}^{n} k_i c_i\right)^{2n};$$

$$\delta_{h(d)} \approx 1/\rho^n;\ \delta_{h(gb)} \approx D^n; \qquad (2)$$

$$\delta_{h(c)} \approx 1/v^{2n};\ \delta_{h(nc)} \approx r/v^n$$

where $n=\frac{1}{2}$ at $\sigma\approx\sigma_{max}$ and $n\approx1$ at $\sigma\gg\sigma_{max}$.

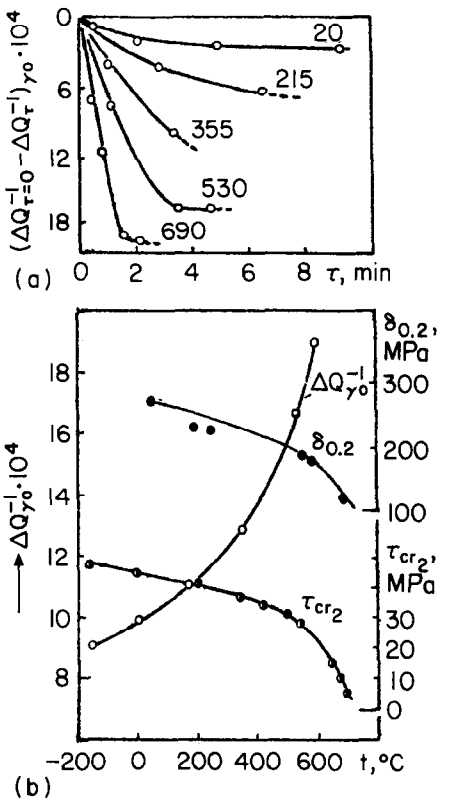

Fig. 5. (a) The influence of T_m and τ_m on ΔQ_0^{-1}. (b) The influence of T_m on ΔQ_0^{-1}, σ_{YS} ($\sigma_{0.2}$) and $\tau_{cr2}=G\gamma_{pr2}$.

TABLE 3. λ_S and δ_{max} as a function of Cr content

Cr content	11–12	15–16	18–20	25
λ_S (10^6)	12	16	14	10
δ_{max} (%)	4–5	8	6	4

The non-monotonic response of ferromagnetic alloys after heat treatment at different temperatures in terms of damping may be attributed to a few partial responses. The resulting IF level due to magnetomechanical hysteresis is the result of the superposition of all the partial contributions to damping.

For dislocation IF, experimental results of ADIF were treated in the axes: tan α *vs.* $1/T$. The critical point between temperature-independent and temperature-dependent ranges of ADIF *vs.* T_m is the temperature of impurity condensation on dislocations ($T^{\perp}$); it depends on the chemical composition. Damping at 500–650 °C is associated with the interference of relaxation (Zener) and hysteresis effects.

The comparison of T_a with $T^{\perp}$ and T_C shows that there are some temperature intervals of additional heat treatment which may increase the damping capacity. The most useful annealing temperature is slightly below T_C, *i.e.* in the range of magnetic domain formation. Prolonged formation of domains leads to the highest damping properties due to: (1) the change in DW

density, width and average domain size and the decrease in the bending energy (DW pinning points), and (2) the additional decrease in σ_i and its gradient.

Annealing around the 475 °C embrittlement temperature produces some peculiarities: short-time annealing increases the IF level; prolonged annealing leads to a large decrease in IF. As a result of annealing for 1 h, a reduction of the concentration of the interstitial solid solution takes place (approximately 70%). The kinetic coefficient of precipitation was calculated using the Wert–Zener equation ($C = C_0 \times \exp[-(\tau/\tau_0)^k]$) and for the first hour of annealing at 475 °C, $k = 0.5$–0.7. This means that the process of dislocation pinning by impurities in Cottrel's atmosphere takes place in this τ_a range. This process is confirmed by the decrease in the tan α ADIF value and is accompanied by a decrease in the width of the X-ray $\beta(1110)$ line, *i.e.* the internal stress decreases.

On prolonged annealing ($\tau > 5$ h), the decomposition of high-Cr ferrite takes place according to the metastable miscibility gap of the Fe–Cr diagram. Decomposition leads to the embrittlement of ferritic steels because of the appearance of zones enriched in Cr and interstitial atom zones (SAS and IF data) (Fig. 6). The increase in the annihilation time of positrons in this case demonstrates the increase in microdistortions in the embrittled structure. After 100 h annealing, the ferritic structure is characterized by the following parameters: density of precipitates, approximately 10^{16}–10^{19} cm^2; Cr concentration, approximately 50%; diameter, 5–10 nm,; microdistortion diameter, approximately 15 nm [7]. The dislocation and DW movement in this Cr-modulated structure is suppressed. This leads to hardening and changes in the magnetomechanical IF as

$$\Delta\sigma_c = h\zeta_0^{3/2}\nu^{1/2}/G^{1/2}D_0^{1/2}b^2\ln(D_0/b)^{1/2}$$
$$\delta_{h(c)} \approx D_0^{1/2}\ln(D_0/b)^{1/2}/v^{1/2}h \quad (3)$$

where h and D_0 are the disc width and diameter and ζ_0 is the interphase surface energy. This leads to the reduction of the IF level due to the increase in the volume fraction of precipitates, *i.e.* the elastic distortions pin DW motion. This effect become predominant with prolonged annealing.

The maxima in the curves Q_0^{-1}, $\Delta f^2/f^2$ and γ_r *vs.* γ_{pr} appear in a deformation range less than the second critical amplitude of the Granato–Lucke string model, *i.e.* there are no residual effects in the crystalline structure and an increase in non-elastic effects takes place because of the redistribution of DW locations. An increase in the IF level under applied tensile stress takes place when $\sigma < \sigma_{cr2}$.

To explain the above maxima of the Q_0^{-1} or γ_r *vs.* γ_{pr} or σ_{st} curves, it is possible to use the same approach [4] as adopted for the same dependence of IF on the value of the external magnetic field. By applying small cyclic stresses, most of the DWs will move reversibly without hardly any energy dissipation. Small mechanical stresses or magnetic fields will shift the DW location from the lowest points to the position where the Relay function is a maximum. Due to this additional stress a part of DW may shift irreversibly. When $\gamma_{pr} < \gamma_Q$, the external mechanical or magnetic field increases the number of irreversible jumps of DWs and lowers the IF level. When $\gamma_{pr} > \gamma_{cr2}$, microplastic deformation appears and leads to a decrease in IF (Q_0^{-1}).

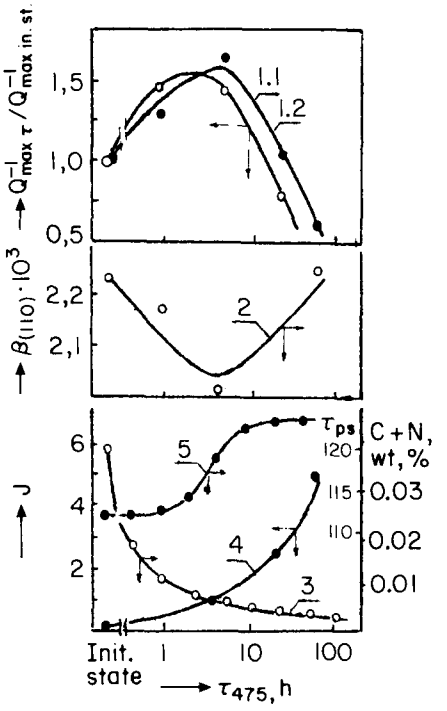

Fig. 6. The influence of annealing time at 475 °C on Q_h^{-1} ($H = 0$) (1.1, Cr16; 1.2, Cr16Mo4), $\beta(110)$ (2), C+N content in the solid solution (3), degree of decomposition in the Fe–Cr system (4) and positron lifetime (5).

References

1 I.S. Golovin, V.I. Sarrak and S.O. Suvorova, *Mater. Sci. Forum, 119–121* (1993) 415–418.
2 A.B. Lebedev and S.B. Kustov, *Phys. Status Solidi A, 116* (1989) 645.
3 Author, *Mater. Sci. Forum, 119–121* (1993) 598–599.
4 I.B. Kekalo, *Met. Sci. Heat Treatment, 7* (1987) 5–88.
5 I.S. Golovin and N.Y. Rochmanov, *Met. Sci. Heat Treatment, 9* (1993) 29–34.
6 N.Y. Rokhmanov and A.F. Sirenko, *Defects, Structure and Properties of Real Solid Bodies,* Kharcow, 1990, pp. 175–195.
7 I.S. Golovin, V.I. Sarrak and S.O. Suvorova, *Metall. Trans. A, 23* (9) (1992) 2567–2579.